Formulation of active food packaging by design: Linking composition of the film-forming solution to properties of the chitosan-based film by response surface methodology (RSM) modelling

Marijan Bajić, Ana Oberlintner, Kristi Kõrge, Blaž Likozar, Uroš Novak

PII: S0141-8130(20)33347-X

DOI: https://doi.org/10.1016/j.ijbiomac.2020.05.186

Reference: BIOMAC 15669

To appear in: *International Journal of Biological Macromolecules*

Received date: 10 April 2020

Revised date: 13 May 2020

Accepted date: 22 May 2020

Please cite this article as: M. Bajić, A. Oberlintner, K. Kõrge, et al., Formulation of active food packaging by design: Linking composition of the film-forming solution to properties of the chitosan-based film by response surface methodology (RSM) modelling, *International Journal of Biological Macromolecules* (2020), https://doi.org/10.1016/j.ijbiomac.2020.05.186

Formulation of active food packaging by design: Linking composition of the film-forming solution to properties of the chitosan-based film by response surface methodology (RSM) modelling

Marijan Bajić [a,b,*], Ana Oberlintner [a], Kristi Kõrge [a,c], Blaž Likozar [a,d], Uroš Novak [a]

[a] Department of Catalysis and Chemical Reaction Engineering, National Institute of Chemistry, Hajdrihova 19, 1000 Ljubljana, Slovenia

[b] Department of Biochemical Engineering, University College London, Gower Street, London WC1E 6BT, United Kingdom (present affiliation)

[c] Department of Chemistry and Biotechnology, Tallinn University of Technology, Akadeemia tee 15, 12618, Tallinn, Estonia

[d] Faculty of Chemistry and Chemical Technology, University of Ljubljana, Večna pot 113, 1000 Ljubljana, Slovenia

Abstract

An active chitosan-based film, blended with the hydrolysable tannin-rich extract obtained from fibrous chestnut wood (*Castanea sativa* Mill.), underwent a simultaneous engineering optimization in terms of measured moisture content (*MC*), tensile strength (*TS*), elongation at break (*EB*), and total phenolic content (*TPC*). The optimal product formulation for a homogeneous film-forming solution was sought by designing an empirical Box–Behnken model simulation, based on three independent variables: the concentrations of chitosan (1.5–2.0% (w/v)), extracted powder-form chestnut extract (0.5–1.0% (w/v)) and plasticizer glycerol (30.0–90.0% (w/w); determined per mass of polysaccharide). Obtained linear (*MC*), quadratic (*TS* or *EB*), and two-factor interaction (*TPC*) sets were found to be significant ($p < 0.05$), to fit well with characteristic experimental data ($0.969 < R^2 < 0.992$), and could be considered predictive. Although all system parameters were influential, the level of polyol played a vital continuous role in defining *EB, MC* and *TS*, while the variation of the chestnut

[*]Corresponding author.
E-mail addresses: marijan.bajic@ki.si; m.bajic@ucl.ac.uk (M. Bajić).

extract caused an expected connected change in affecting *TPC*. The component relationship formula of chemical mixture fractions (1.93% (w/v) of chitosan, 0.97% (w/v) chestnut extract and 30.0% (w/w) of glycerol) yielded the final applicable material of adequate physico-mechanical properties (*MC* = 17.0%, *TS* = 16.7 MPa, *EB* = 10.4%, and *TPC* = 19.4 mg_{GAE} g_{film}^{-1}). Further statistical validation of the concept revealed a sufficient specific accuracy with the computed maximal absolute residual error up to 22.2%. Herein-proposed design methodology can thus be translated to smart packaging fabrication generally.

Keywords: active chitosan-based film; chestnut wood extract; Box–Behnken experimental design methodology; bio-based film-forming solution; physico-mechanical properties; simultaneous model-based optimization

1. Introduction

The history of chitosan dates back to the mid-19th century, although its industrial production and utilization start from the 1970s [1]. Nowadays, a quest for novel methods of chitosan extraction, modification, and characterization is in full swing [2,3]. This trend is based on the facts that chitosan is a non-toxic, biodegradable, and biocompatible biopolymer with a good film-forming capacity as well as inherent antimicrobial and antioxidant activities [4,5]. Following this, chitosan has been placed in focus as prospective raw material for the preparation of eco-friendly films for food packaging applications [6–8]. Chitosan-based films, however, may require the incorporation of certain auxiliary components to ameliorate functional properties. In the first instance, plasticization is done to minimize the films' rigidness and brittleness [9], whereby polyols (most of all glycerol) stand as the most widely used plasticizers [10,11]. On the other hand, the incorporation of various active components can lead to the production of chitosan-based films with the enhanced mechanical, barrier, and antimicrobial and/or antioxidant properties [3,7,12].

Extracts obtained from different parts of terrestrial plants are frequently used active components in eco-friendly films [13]. Recent studies on chitosan-based films highlight the utilization of extracts obtained from banana [14], mangosteen [15], mango [16], black plum [17], pine/peanut/jujube [18], turmeric [19], hop [20], oak [21], and chestnut [22]. The extract obtained from chestnut wood is quite complex in composition but its major fraction consists of hydrolyzable tannins (HTs), while other components include water, ellagic/gallic acids, simple sugars, proteins, mineral substances, and crude fibre [23]. HTs are secondary plant metabolites, but also phenolic compounds by their chemical nature [24]. Due to their prominent biological activity, HTs-rich chestnut extracts have found applications beyond the border of their traditional use in tanning, e.g. as an active agent in the food industry [25,26].

The above-mentioned auxiliary components (plasticizers, active agents) are usually pre-added in the film-forming solutions (FFSs), which could be considered as the films' semi-finished products. The further strategy of the film production means casting of homogeneous FFSs on a flat surface followed by a time-limited process of solvent evaporation at moderate temperatures [6]. The auxiliary components affect the biological and physico-chemical characteristics of resulting films

interdependently, and thus the formulation of FFSs should be carefully optimized in terms of achieving desired properties of the final products. A set of statistical and mathematical tools known as RSM is of great importance in the design, development, and optimization of new as well as in the improvement of existing products [27]. For instance, a family of efficient three-level Box–Behnken design, BBD [28], has been applied for the development of either pure or blended chitosan-based films in several studies. Drying temperature seems to be the most frequently studied independent variable, either in combination with other process parameters (e.g. relative humidity, storage period [29]) or with film composition parameters (e.g. chitosan/glycerol level [30], glycerol/vanillin level [31]). On the other hand, BBD has been used to optimize only the formulation of chitosan-containing composite films blended with TiO_2 [32], pea starch [33], and cellulose/polyvinyl alcohol [34].

This study brings the optimization of novel active chestnut extract-incorporated chitosan-based film intended for food packaging into the foreground, and therefore represents an extension of our previous work on it [22]. The simultaneous optimization was done by linking the composition of the FFS containing matrix-forming biopolymer (chitosan), active component (chestnut extract), and plasticizer (glycerol) to the properties of the active film material. Individual and interactive effects of the independent variables (concentrations of the FFS components) on the response variables (*MC*, *TS*, *EB*, and *TPC* of the film material) were evaluated by RSM. Moreover, model validation was done by comparing predicted values of the response variables with those obtained from the experimental measurements.

2. Materials and methods

2.1. Materials

High molecular weight chitosan (M_w = 310-375 kDa; deacetylation degree ≥ 75%), lactic acid (purity >85%; density 1.206 g mL^{-1}), Folin-Ciocalteu's phenol reagent, magnesium nitrate, and gallic acid were purchased from Sigma-Aldrich (Steinheim, Germany). Sodium carbonate and glycerol were from Merck (Darmstadt, Germany) and Pharmachem Sušnik (Ljubljana, Slovenia), respectively. All chemicals except lactic acid were of analytical grade. Milli-Q® water was used throughout all experiments.

Tanin Sevnica (Sevnica, Slovenia) kindly donated a commercially available chestnut extract obtained from individual parts of chestnut wood. The extract contained ≥75% of tannins and <4% of ash [22], according to the manufacturer's specifications.

2.2. Experimental design

A 3-level-3-factor BBD with three replicates at the central point, which gives a total of 15 experimental runs [29,31–33], was used to study the effect of FFS composition on the physico-mechanical properties of chitosan-based films (prepared according to the protocols described in Section 2.3). The levels of three main components of the FFS were chosen as independent variables: (i) concentration of chitosan (CH, x_1, % w/v), (ii) concentration of chestnut extract (CE, x_2, % w/v), and (iii) concentration of glycerol (GLY, x_3, % w/w, calculated per mass of chitosan); whereby each variable was tested at three different coded levels: low (–1), medium (0), and high (+1). The low level was limited by mechanical properties of the final materials (films prepared from the FFSs containing a low amount of raw materials tend to be mechanically unstable and brittle), while the high level was limited by physical properties of the FFSs (the addition of raw materials in high concentrations gives very viscous and inapplicable FFSs). The experimental design matrix, in terms of actual (x_i) and coded (X_i) levels of the independent variables, is presented in Table 1.

Table 1. Box−Behnken experimental design matrix.

Run	Actual values*			Coded values**		
	x_1	x_2	x_3	X_1	X_2	X_3
1	1.50	0.50	60	–1	–1	0
2	2.00	0.50	60	+1	–1	0
3	1.50	1.00	60	–1	+1	0
4	2.00	1.00	60	+1	+1	0
5	1.50	0.75	30	–1	0	–1
6	2.00	0.75	30	+1	0	–1
7	1.50	0.75	90	–1	0	+1
8	2.00	0.75	90	+1	0	+1
9	1.75	0.50	30	0	–1	–1
10	1.75	1.00	30	0	+1	–1
11	1.75	0.50	90	0	–1	+1
12	1.75	1.00	90	0	+1	+1
13	1.75	0.75	60	0	0	0
14	1.75	0.75	60	0	0	0
15	1.75	0.75	60	0	0	0

*Actual values: x_1 – concentration of chitosan (CH, % w/v); x_2 – concentration of chestnut extract (CE, % w/v); x_3 – concentration of glycerol
(GLY, % w/w; calculated per mass of chitosan). The concentration of lactic acid was kept constant, as stated in Section 2.3.1.

**Coded values: X_1 – the coded level of CH; X_2 – the coded level of CE; X_3 – the coded level of GLY.

The coded values are related to the actual values by the relation indicated in Eq. 1:

$$X_i = 2 \times (x_i - x_m) / d_i \quad (1)$$

whereby x_i, x_m, and d_i denote variable value in the actual units of the ith observation, mean of the highest and the lowest variable value, and the difference between the highest and the lowest variable value, respectively [30]. After conducting all experimental runs (Table 1), a second-order polynomial equation was applied to fit the experimental responses to the coded variables, as denoted in Eq. 2:

$$Y_n = \beta_0 + \sum_{i=1}^{3} \beta_i X_i + \sum_{\substack{i=1 \\ i<j}}^{3} \sum_{i=1}^{3} \beta_{ij} X_i X_j + \sum_{i=1}^{3} \beta_{ii} X_i^2 + \varepsilon \quad (2)$$

where,

Y_n denotes predicted response;

X_i (X_j) denotes a dimensionless coded value of the independent variable x_i (x_j);

β_0 denotes the model constant (intercept);

β_i denotes linear regression coefficient;

β_{ij} denotes cross-product regression coefficient;

β_{ii} denotes quadratic regression coefficient.

2.3. Film-forming solutions and chitosan-based films

2.3.1. Film-forming solutions

All FFSs formulations (Table 1) were prepared by adding predetermined amounts of CH (% w/v) and GLY (% w/w, calculated per mass of CH) in the solvent (1% (v/v) aqueous solution of lactic acid) followed by continuous stirring (1000 rpm; 12 h; room temperature, 24 °C) on RCT magnetic stirrer (IKA, Staufen, Germany) and vacuum-filtration through two sheets of medical gauze [20]. The predetermined amounts of CE were added subsequently after the filtration step and the mixtures were homogenized (6000 rpm; 2 min) on Ultra-Turrax® T50 (IKA) and left overnight to get rid of the air bubbles formed during this process. A small amount of stable sticky foam that was formed on the top of the mixtures due to the presence of CE was eventually removed by using a laboratory spatula [22]. A potential loss of CE during this procedure was presumed to be insignificant and without influence on the qualitative and quantitative composition of the FFSs.

2.3.2. Chitosan-based films

Prepared FFSs were cast in polyurethane Petri dishes (approximately 0.32 mL cm^{-2}) and left in drying oven Kambič SP-55 C (Kambič, Semič, Slovenia) at 40 °C for the next 48 h. Obtained films were peeled off from Petri dishes, treated by ABS Digital Thickness Gauge (Mitutoyo, Aurora, USA) to measure their thicknesses (the measurements were performed at ten randomly selected positions and the results were averaged), and stored in a glass humidity chamber containing a saturated aqueous solution of $Mg(NO_3)_2$ (relative humidity, RH = 53–55%; room temperature, 24 °C) until further analysis.

2.4. Fourier transform infrared spectroscopy analysis

The Fourier transform infrared (FT-IR) spectra (wavenumbers range from 4000 cm^{-1} to 450 cm^{-1}; resolution 4 cm^{-1}) were recorded at room temperature using Spectrum Two FT-IR spectrometer (PerkinElmer, Waltham, USA). The tested film samples were prepared from the FFSs containing 1.5% (w/v) of CH (unplasticized film), 1.5% (w/v) of CH and 30.0% (w/w; per mass of chitosan) of GLY (plasticized film), and 1.5% (w/v) of CH, 30.0% (w/w; per mass of chitosan) of GLY, and 1.0% (w/v) of CE (plasticized film with incorporated CE). The scans were done in triplicates on random positions of each tested sample and the resulting curves were averaged.

2.5. Response variables

2.5.1. Moisture content

MC was determined gravimetrically, according to the previously described protocol [20]. In short, rectangular samples (~1 cm^2) were weighted on an analytical balance (Kern & Sohn, Balingen, Germany) to get the initial (M_1) and dry mass (M_2; obtained after drying at 105 ℃ for 24 h), and the results were expressed as the percentage of water content in the films following that $MC = (M_1 - M_2 / M_1) \times 100\%$.

2.5.2. Tensile strength

TS was determined by testing rectangular film samples (length × width = 8 cm × 2 cm; gage length segment 6 cm) on the XLW Auto Tensile Tester (Labthink® Instruments, Jinan, China) equipped with a 100 N load cell, at a crosshead speed of 25 mm min^{-1}. *TS* was calculated by dividing the maximal load with the average original cross-sectional area in the sample gage length segment [20].

2.5.3. Elongation at break

EB was tested on the same samples and using the same equipment as stated in Section 2.5.2. *EB* was calculated as the ratio between increased length after breakage and the initial gage length [20].

2.5.4. Total phenolic content

TPC was estimated using Folin-Ciocalteu´s (FC) phenol reagent, as described elsewhere [20]. Small rectangular film samples of known masses were placed in glass vials, and water was added to reach the final film concentration of 5 mg mL^{-1}, followed by successive addition of FC phenol reagent and 10% (w/v) aqueous solution of Na_2CO_3 (added 10% and 20% based on the volume of water, respectively). After the sample incubation for 2 h (dark conditions; room temperature), the absorbance of the solutions was measured at 765 nm using Synergy™ 2 Multi-Detection Microplate Reader (BioTek, Winooski, USA). The results were expressed as the mass of gallic acid equivalent (GAE) per mass of the film.

2.6. Simultaneous optimization and model validation

A desirability function-based approach [27] was used for the simultaneous optimization of response variables (Eq. S1, Appendix A). The optimization was done based on the following goals: (i) minimization of *MC*, (ii) maximization of *TS*, (iii) minimization of *EB*, (iv) maximization of *TPC*. An algorithm was then applied to maximize the overall desirability (*D*; ranging from 0 to 1), defined as the geometric average of the individual desirability functions [31]. Model validation was performed by comparing predicted values of the response variables and those obtained from experimental measurements using a set of films prepared from the optimized FFS.

2.7. Statistical analysis

All measurements (Sections 2.5.1–2.5.4) on the film samples prepared for tested FFSs (runs 1–15, Table 1) were performed in triplicates and the mean values were used in the analysis. Statistical analysis and simultaneous optimization were done by a trial version of Design-Expert® software (Stat-Ease, Minneapolis, USA; version 12.0.0.6; serial number: 7614-9562-2103-EVAL). Response surface graphs obtained from the regression equations in terms of coded values were visualized using a Python plotting library Matplotlib.

3. Results and discussion

3.1. Preparation of film-forming solutions and chitosan-based films

Two raw materials used in this study – the matrix-forming biopolymer CH (Figure 1a) and the active component CE (Figure 1b) – are obtainable from natural and renewable sources such as marine- and wood-based biomass, respectively. The third raw material, plasticizer GLY, was added in a low concentration relative to CH and CE, but it was very influential on the film properties (Sections 3.3–3.5). Processing of the raw materials led to the preparation of brown-shaded FFSs (Figure 1c), whose formulation was further optimized to get films of satisfying mechanical integrity and desired physico-mechanical properties (Figure 1d).

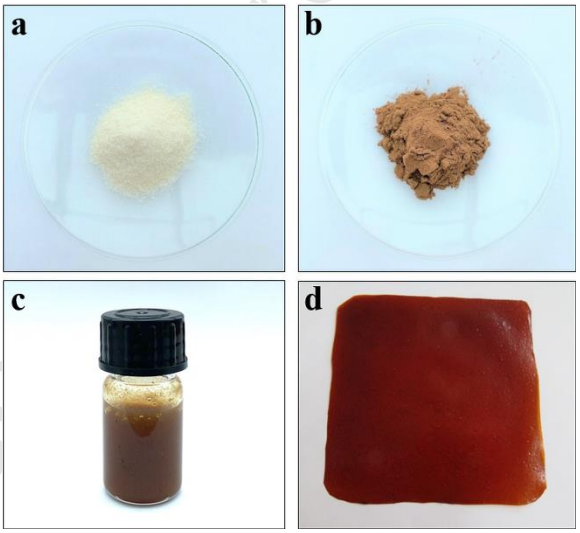

Fig. 1. The physical appearance of a) chitosan powder, b) chestnut extract powder, c) film-forming solution containing chestnut extract, and d) chitosan-based film prepared from the film-forming solution containing the chestnut extract.

It has been visually observed that variation in the concentrations of raw materials significantly affects the physical properties of the FFSs. In this regard, the viscosity of FFSs was mainly affected by variations in the concentrations of CH and CE, while their visual appearances were affected by

variations in the concentration of CE. A brownish shade of FFSs became more intense upon increasing the concentration of CE (Fig. S1, Appendix A), whereby this trend was replicated in the visual appearance of chitosan-based films as well (Fig. S2, Appendix A).

The morphological evaluation of film materials has revealed their compact structure without any significant microscopic pores or cracks at the films' cross-sections and surfaces (Fig. S2, Appendix A). The mean thickness of all tested film samples (Section 2.2) was 120 ± 30 µm, which is slightly above the values obtained for our previous chitosan-based films prepared from the FFSs containing up to 1.5% (w/v) of hop extract [20]. Nevertheless, it is still within the range of values for other chitosan-based films with incorporated active components [16,18].

3.2. Fourier transform infrared spectroscopy analysis

Towards a better understanding of the relationship between the qualitative composition and possible interactions/structural changes after the film formation, the FT-IR analysis of unplasticized, plasticized, and plasticized films with incorporated CE has been done (Fig. 2).

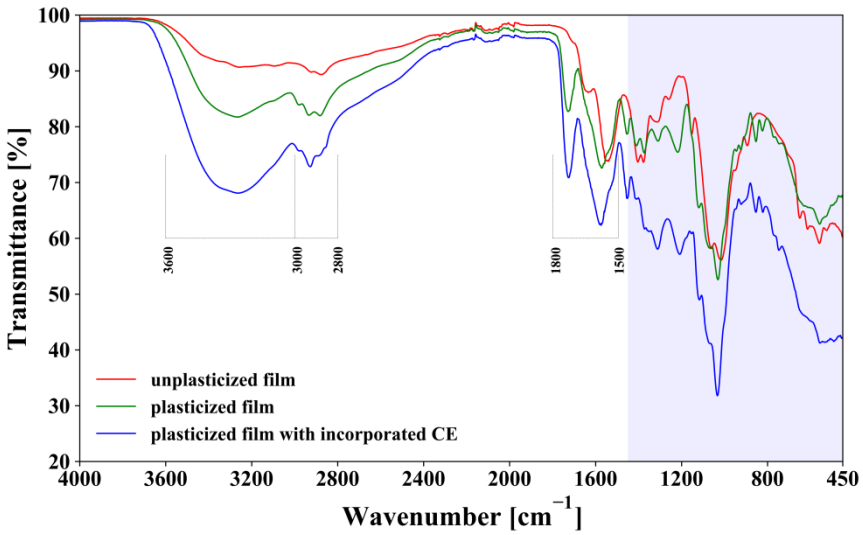

Fig. 2. FT-IR spectra of chitosan-based films prepared from the film-forming solutions containing 1.5% (w/v) of CH (unplasticized film; red line), 1.5% (w/v) of CH and 30.0% (w/w; per mass of chitosan) of GLY (plasticized film; green line), and 1.5% (w/v) of CH, 30.0% (w/w; per mass of

chitosan) of GLY, and 1.0% (w/v) of CE (plasticized film with incorporated chestnut extract; blue line). The grey-shaded area represents the fingerprint region.

The most characteristic absorption bands in unplasticized films are as follows: a broad band in the wavelength region between 3600 cm^{-1} and 3000 cm^{-1} (attributed to O–H and N–H stretching), two weak bands located approximately between 2950 cm^{-1} and 2850 cm^{-1} (attributed to C–H stretching), and the peaks appearing at around 1640 cm^{-1} and 1550 cm^{-1} attributed to C=O stretching (amide I) and N–H bending (amide II), respectively (Fig. 2). This spectrum is generally in keeping with the spectrum of a similar neat chitosan-based film [35].

Plasticization of chitosan film utilizing GLY and its further incorporation by CE brought about certain alterations in the FT-IR spectra. The most distinctive changes are visible in the wavelength regions between 3600–3000 cm^{-1} (higher intensity of broad bands), 3000–2800 cm^{-1} (higher intensity of peaks at approx. 2930 cm^{-1}), and 1800–1490 cm^{-1} (higher intensity of sharp peaks at approx. 1728 cm^{-1} and 1570 cm^{-1} followed by a slight shift towards higher wavenumbers as compared to the unplasticized film). Such changes might indicate the interactions of chitosan's O–H, C=O (amide I), and N–H (amide II) groups with the main functional groups of auxiliary components. For instance, GLY has been commonly reported to promote hydrogen bonding with chitosan due to a strong hydrogen bond capacity promoted by the presence of three O–H groups [9,36], which is per its role as a plasticizer. On the other hand, the main fraction of CE is composed of HTs – a mixture of structurally distinct compounds (such as simple gallic acid derivatives, gallotannins, and ellagitannins) that possess a huge number of O–H (and C=O) functional groups [24]. It could be assumed that these functional groups are also involved in the non-covalent interactions with CH molecules. This assumption might be supported by similar changes in the FT-IR spectrum of a chitosan-based film with incorporated ellagitannins-rich oak extract [21], which belongs to the same class as CE [37].

General conclusions derived from the FT-IR spectra of herein presented three representative samples of chitosan-based films might point to good incorporation of the auxiliary components in the polymer matrix established over non-covalent interactions of GLY and HTs with O–H, N–H, and

C=O (in acetylated monomers) groups of CH. Nevertheless, the FT-IR analysis has not been intended to play a decisive role in whether (and how) the interactions between components reflect at the final properties of chitosan-based films. This analysis actually should play a supportive role, i.e. the results from this section should be interpreted in context with the models discussed below. For those who seek a more detailed spectroscopic analysis, the FT-IR spectra of raw materials are enclosed in Appendix A (Fig. S3), whilst a more in-depth interpretation can be found elsewhere in the literature [10,35,37].

3.3. Moisture content

MC notably affects the barrier, mechanical, and thermal properties of chitosan-based films, which is of paramount importance for their application in food preservation [38]. Therefore, a set of 15 experimental measurements conducted on this variable revealed that *MC* was ranging from 20.2% to 42.8% (Table 2).

Table 2. Experimental responses of dependent variables.

Run[*]	**Experimental response**[**]			
	MC	***TS***	***EB***	***TPC***
1	35.1	7.7	53.7	13.0
2	33.4	8.7	56.9	10.1
3	25.1	10.4	62.4	22.9
4	28.5	7.8	23.4	19.9
5	21.7	21.6	48.1	17.4
6	20.4	18.0	10.3	19.0
7	38.6	5.6	59.3	17.7
8	36.3	6.6	57.6	12.6
9	24.8	14.7	57.1	11.0
10	20.2	15.7	36.7	23.7
11	42.8	4.4	86.7	9.6
12	36.5	3.2	68.3	17.8
13	30.4	9.7	75.0	16.2
14	31.1	7.1	71.8	17.1
15	30.7	8.2	69.6	14.5
Min.	20.2	3.2	10.3	9.6
Max.	42.8	21.6	86.7	23.7

Mean	30.4	10.0	55.8	16.2
Std. Dev.	6.7	5.1	19.2	4.2

*The actual and coded values of independent variables in each experimental run are presented in Table 1.

***MC*, moisture content (%); *TS*, tensile strength (MPa); *EB*, elongation at break (%); *TPC*, total phenolic content ($mg_{GAE}\ g_{film}^{-1}$).

Further processing of the experimental data has led to the development of a linear mathematical model which efficiently described the relationship between independent variables and *MC* [$Y_{MC} = 30.37 - 0.24X_1 - 3.23X_2 + 8.39X_3$]. An insight into the ANOVA summary statistics implied the model was significant (Table 3), whereby the proposed equation matched at least 96.85% of the total variations. Furthermore, a small difference between R^2 and adjusted R^2 (R^2_{adj}) indicated there were no unnecessary model terms included [27].

Table 3. ANOVA summary statistics.

Response*	Source	*SS***	*df***	*MS***	*F*-value	*p*-value	R^2	R^2_{adj}**	Remark
MC	Model	646.46	3	215.49	112.81	< 0.0001	0.9685	0.9599	Linear model
	Lack of fit	20.77	9	2.31	18.71	0.0518			
TS	Model	378.68	9	42.08	31.51	0.0007	0.9827	0.9515	Quadratic model
	Lack of fit	3.27	3	1.09	0.64	0.6572			
EB	Model	5494.74	9	610.53	72.91	< 0.0001	0.9924	0.9788	Quadratic model
	Lack of fit	27.12	3	9.04	1.23	0.4786			
TPC	Model	255.82	6	42.64	43.78	< 0.0001	0.9704	0.9483	2FI model
	Lack of fit	4.30	6	0.7174	0.4115	0.8314			

**MC*, moisture content (%); *TS*, tensile strength (MPa); *EB*, elongation at break (%); *TPC*, total phenolic content ($mg_{GAE}\ g_{film}^{-1}$).

***SS*, the sum of squares; *df*, degrees of freedom; *MS*, mean square; R^2_{adj}, adjusted R^2.

In this case, concentrations of CE and GLY were significant model terms ($p < 0.05$). The effect of all three independent variables on *MC* can be seen in Fig. 3a.1−3a.3. *MC* was almost constant along with the entire range of CH concentrations, but the values increased along with decreasing amount of CE (Fig. 3a.1), and the increasing amount of GLY (Fig. 3a.2). Plotting the concentrations of active component and plasticizer showed the highest values of *MC* were in the films produced from the FFS containing the minimal concentration of CE and maximal concentration of GLY (Fig. 3a.3).

Such a response might be a consequence of the hydrogen bonding between CH and auxiliary components. Namely, GLY establishes intermolecular hydrogen bonds with adjacent chains of CH (Section 3.2), causing changes in the spatial conformation of the film three-dimensional matrix [9,36].

This might as well expose hydrogen bonding sites of CH to interact with water molecules and retain them within the polymer matrix. The fact that GLY is hygroscopic by itself due to the presence of three −OH could be contributive to *MC* as well [33]. A positive correlation between the level of GLY and *MC* in chitosan-based films is in line with the findings reported elsewhere [10,33]. On the other hand, CE was added in much higher concentrations relative to GLY. Its major components (HTs) possess multiple interaction sites that crosslink polymer chains and therefore tend to saturate hydrogen bonding sites of CH. This might further prevent the retention of water molecule within the matrix and lead to lower values of *MC*. The incorporation of other plant-based active components has also been reported to reduce the water absorption capacity of chitosan-based films [15,16,20].

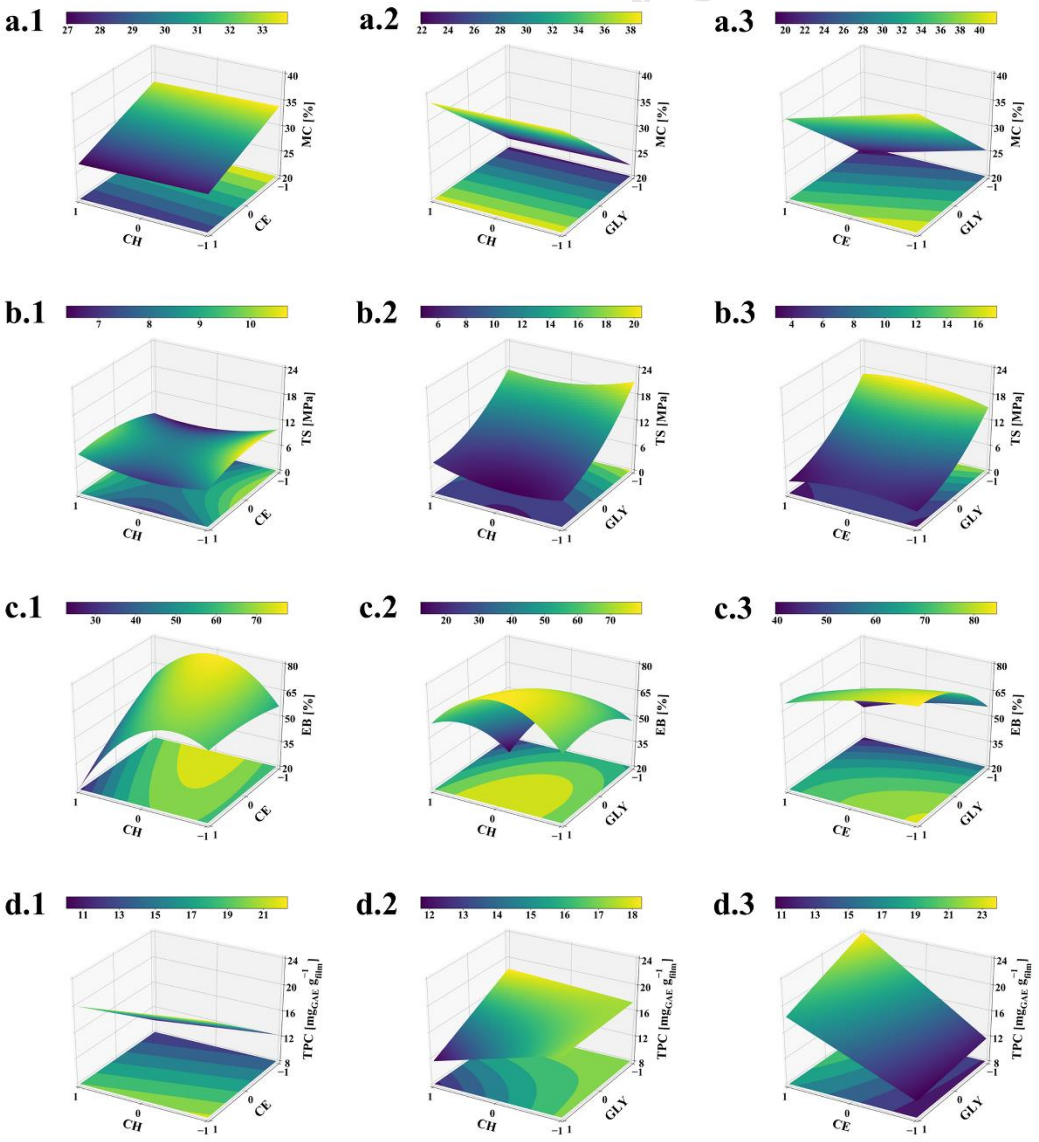

Fig. 3. Response surface plots showing the impact of independent variables on: a) moisture content, b) tensile strength, c) elongation at break, and d) total phenolic content of chitosan-based films. The numbers 1, 2, and 3 denote the mutual effect of CH–CE while the level of GLY was held constant, the mutual effect of CH–GLY while the level of CE was held constant, and the mutual effect of CE–GLY while the level of CH was held constant, respectively. Corresponding two-dimensional contour plots can be seen in Appendix A (Fig. S4).

3.4. Tensile strength

TS represents one of the most studied mechanical property of chitosan-based films intended for food packaging, and it refers to the films' resistance to failure at elevated loads or deformation. The values of *TS* should be as high as possible because food packaging must preserve mechanical integrity and therefore provide sufficient protection of the food during transportation and storage. The *TS* values of tested film samples were ranging from 3.2 MPa to 21.6 MPa (Table 2), which is in agreement with the values of many other biodegradable packaging films with incorporated plant extracts [13], but slightly below the values of some frequently used commercial materials [39]. The relationship between the independent variables and *TS* was found to be quadratic [$Y_{TS} = 8.33 - 0.53X_1 + 0.20X_2 - 6.28X_3 - 0.90X_1X_2 + 1.15X_1X_3 - 0.55X_2X_3 + 1.88X_1^2 - 1.57X_2^2 + 2.73X_3^2$]. As can be seen from Table 3, this equation could describe at least 98.27% of the total variations, while the model and lack of fit *F*-values imply significance and good fit of the model, respectively.

TS of the samples was likely governed by physical interactions established between CH molecules, the vast majority of CE components, and GLY (as discussed in Section 3.2). It was found that *TS* was significantly ($p < 0.05$) affected by GLY level (in linear and quadratic terms), while the levels of CH and CE found to be influential as well, but less dramatically and mostly in quadratic terms. This can be observed from the response plots − *TS* slightly varied along with the variations of CH and CE levels (Fig. 3b.1), but it steeply decreased with increasing the concentration of plasticizer, with the values below 10 MPa in the films prepared from the FFSs containing maximal concentrations of GLY (Fig. 3b.2 and 3b.3). This was in line with a well-known fact about the remarkable plasticization effect of GLY due to high hydrogen-bonding capacity [9,10]. However, the level of GLY significantly

affected *MC* as well (Section 3.3), and in return, *MC* affects the mechanical properties of chitosan-based films [38]. So we might assume there were more water molecules absorbed in the polymer matrix than it would have happened in the absence of GLY. It can be further concluded that these water molecules exhibit a joint plasticization effect with GLY. This effect is very likely 'masked' in this model, and should not be neglected or excluded when considering mechanical properties of chitosan-based films.

3.5. Elongation at break

EB is another important mechanical property of chitosan-based films, and it stands for their stretching capacity (i.e. extensibility) before breaking. The obtained values were between 10.3% and 86.7% (Table 2), which falls in the range reported for other plant extract-blended biopolymer films [13]. For comparison's sake, the presented chitosan-based films had higher *EB* values than polystyrene (PS; 1% − 4%) and polyamide (PA; 5% − 10%), smaller than low-density polyethylene (LDPE; 200% − 900%), polyvinyl alcohol (PVA; 220% − 250%) and polyvinyl alcohol-co-ethylene (EVOH; 180% − 250%), while their *EB* values fell in the range of polyethylene terephthalate (PET; 20% − 300%) and polyvinyl chloride (PVC; 40% − 75%) [39].

The model, which could describe at least 99.24% of the total variations (Table 3), revealed a quadratic relationship between *EB* and independent variables [$Y_{EB} = 72.13 - 9.41X_1 - 7.95X_2 + 14.96X_3 - 10.55X_1X_2 + 9.03X_1X_3 + 0.50X_2X_3 - 20.70X_1^2 - 2.33X_2^2 - 7.60X_3^2$]. A perusal of Table 3 shows there was a reasonable agreement between the ordinary and adjusted R^2, while observation of the *F*-values implies the model was significant. All three independent variables exerted significant ($p < 0.05$) influence on *EB* in linear, interaction (excepted CE and GLY), and quadratic (excepted CE) terms. As evident from the model equation, levels of CH and CE were in negative correlations with *EB* in all three terms, i.e. the flexibility of films decreased in a non-linear manner at elevated concentrations of CH and CE − most probably due to extensive cross-linking between CH polymer and HTs from chestnut extract (Section 3.2). This could be seen on the response plot, where the lowest *EB* values were predicted for the films produced from the FFSs with maximal concentrations of CH and CE (lower-left corner of the plot in Fig. 3c.1). On the other hand, the plasticization effect

of GLY was evident since the films' elongation capabilities increased along with increasing the concentration of GLY, with the highest *EB* values around mid-level of CH (Fig. 3c.2) and the minimal level of CE (Fig. 3c.3). This trend was in line with the results of *TS* (Section 3.4) since it is expected that *TS* and *EB* have a linear, inversely proportional relationship due to plasticization by GLY [9]. The same relationship was confirmed in this study by plotting model-predicted *TS* and *EB* values as a function of GLY level (Fig. S5, Appendix A).

3.6. Total phenolic content

Natural antioxidants are common active components in sustainable food packaging systems due to their prominent role in the scavenging of oxidation inducers [21 and ref. therein]. HTs from CE retained their antioxidant activity after the incorporation in chitosan-based film, while their potential for scavenging free radicals was in a positive correlation with *TPC* [22]. This is the reason why the *TPC* of the given chitosan-based films was chosen as a relevant parameter to be optimized together with *MC* and mechanical properties. Following this, the *TPC* values in the studied film samples were ranging from 9.6 $mg_{GAE}\ g_{film}^{-1}$ to 23.7 $mg_{GAE}\ g_{film}^{-1}$ (Table 2). For instance, *TPC* values in chitosan-based films prepared from different FFSs containing a banana peels extract, a hop extract, and a mango leaf extract were up to ~4.8 $mg_{GAE}\ g_{film}^{-1}$ [14], up to ~12.7 $mg_{GAE}\ g_{film}^{-1}$ [20], and up to ~12.8 $mg_{GAE}\ g_{film}^{-1}$ [16], respectively.

It was revealed that the relation between *TPC* and independent variables was best described by a two-factor interaction (2FI) model [$Y_{TPC} = 16.17 - 1.18X_1 + 5.07X_2 - 1.68X_3 - 0.03X_1X_2 - 1.68X_1X_3 - 1.12X_2X_3$]. The 2FI model does not have quadratic terms which indicates that CH–CH, CE–CE, and GLY–GLY interactions did not affect *TPC*. Based on the parameters presented in Table 3, it was possible to conclude the proposed equation fitted the experimental data very well and the model was significant. As expected, the most influential variable was the concentration of CE (linear term), which exhibited a strong positive correlation with *TPC*. A steep slope in the response plot was observed along with the increase of the extract concentration, whereby the films prepared from the FFSs with the maximal concentration of CE tended to have *TPC* values higher than 15 $mg_{GAE}\ g_{film}^{-1}$ (Fig. 3d.1 and 3d.3). Considering the effect of CH and GLY levels, the highest values of *TPC* tended

to be in the films prepared from the FFSs with the maximal concentration of CH and the minimal concentration of GLY (Fig. 3d.2). This is most likely because chitosan-based films can exhibit certain *TPC* values due to the reaction of FC reagent with $–NH_2$ groups from the polymer molecules [20 and ref. therein]. These functional groups were probably occupied upon the increase of GLY level and therefore became inaccessible for FC regent resulting in a decline of *TPC* at higher concentrations of plasticizer eventually.

3.7. Simultaneous optimization and model validation

The results presented throughout Sections 3.3–3.6 testified that the evaluated independent variables were mutually competitive. Simultaneous optimization of four variables that govern the films' physico-mechanical properties is thus not always an easy task since it implies a compromise between different attributes of the final material. Besides, the definition of desired attributes of the final material is a subjective matter made by a decision-maker, whereby the authors of this study were guided by the fact this material might be used for the production of sachets for packaging and storage of food [22]. Following this, the process of simultaneous optimization was done to find the optimal formulation of FFS that could be used to get film material of high gas barrier capabilities, mechanical stability, and antioxidant capacity. In the light of hereto evaluated film properties, it implies minimization of *MC* and *EB* as well as maximization of *TS* and *TPC* as the optimization criteria (Section 2.6).

The numerical solution within the constraints of the model was calculated by Design-Expert® software employing desirability function-based approach. The optimal composition of the FFS in terms of actual values of the raw materials was determined to be 1.93% (w/v) of CH, 0.97% (w/v) of CE, and 30.0% of GLY (w/w; per mass of chitosan), whereby the overall desirability was 0.912. Validation of the model was made by comparison of predicted values with those obtained by experimental evaluation of a new set of film materials prepared from the optimal FFS according to the protocol stated in Section 2.3.2. As evident from Table 4, the absolute residual errors were between 1.0% and 11.2%, which is in line with the accuracy of the models generated for other polymer-based films [31,33,40].

Table 4. Predicted and experimental responses of the films prepared using the optimal FFS formulation.

Response[*]	Predicted value[**]	Experimental value (n = 3)[***]	Absolute residual error (%)[****]
MC	18.9	17.0 ± 0.6	11.2
TS	16.0	16.7 ± 1.3	4.2
EB	10.3	10.4 ± 4.0	1.0
TPC	23.7	19.4 ± 0.1	22.2

[*] *MC*, moisture content (%); *TS*, tensile strength (MPa); *EB*, elongation at break (%); *TPC*, total phenolic content ($mg_{GAE}\ g_{film}^{-1}$).

[**] Predicted values obtained from the model equations.

[***] Experimental values obtained for the chitosan-based film prepared using the optimal FFS (according to the protocol stated in Section 2.3.2).

[****] Absolute residual error (%) = [(experimental value – predicted value)/experimental value] × 100 [40].

4. Conclusions

The response surface methodology has been successfully applied in the formulation of active food packaging by linking composition of the film-forming solution to the physico-mechanical properties of the final material. The results revealed that, among the tested independent variables, the level of plasticizer was the most influential on moisture content and mechanical properties, while the level of the active component was the most influential on the antioxidant capacity of chitosan-based films. Further insight into the optimization and validation of the model-based results showed that it was possible to produce a material with satisfactory moisture, mechanical stability, and antioxidant capacity from the optimized film-forming solution under defined fabrication process parameters. The achievements of this study undoubtedly proved the response surface methodology as a time-saving and cost-efficient tool in design, development, and optimization of active chitosan-based films intended for food packaging.

Conflicts of interest

The authors declare no conflict of interest.

Acknowledgements

BioApp project (Interreg V-A Italy-Slovenia 2014-2020 program) and Slovenian Research Agency (research core funding No. P2-0152) are highly acknowledged for financial support. The authors are grateful to the company Tanin Sevnica (Sevnica, Slovenia) for the donation of chestnut extract.

References

[1] G. Crini, Historical review on chitin and chitosan biopolymers, Environ. Chem. Lett. 17 (2019) 1623–1643.

[2] H. El Knidri, R. Belaabed, A. Addaou, A. Laajeb, A. Lahsini, Extraction, chemical modification and characterization of chitin and chitosan, Int. J. Biol. Macromol. 120 (2018) 1181–1189.

[3] U. Novak, M. Bajić, K. Kõrge, A. Oberlintner, J. Murn, K. Lokar, K.V. Triler, B. Likozar, From waste/residual marine biomass to active biopolymer-based packaging film materials for food industry applications – a review, Phys. Sci. Rev. (2019), https://doi.org/10.1515/psr-2019-0099.

[4] M. Hosseinnejad, S.M. Jafari, Evaluation of different factors affecting antimicrobial properties of chitosan, Int. J. Biol. Macromol. 85 (2016) 467–475.

[5] P. Kulawik, E. Jamróz, F. Özogul, Chitosan role for shelf-life extension of seafood, Environ. Chem. Lett. (2020) 61–74.

[6] P. Cazón, M. Vázquez, Applications of chitosan as food packaging materials, in: G. Crini, E. Lichtfouse (Eds.), Sustain. Agric. Rev., Springer Nature Switzerland AG, Cham, 2019: pp. 81–123.

[7] M. Mujtaba, R.E. Morsi, G. Kerch, M.Z. Elsabee, M. Kaya, J. Labidi, K.M. Khawar, Current advancements in chitosan-based film production for food technology; A review, Int. J. Biol. Macromol. 121 (2019) 889–904.

[8] H. Wang, J. Qian, F. Ding, Emerging chitosan-based films for food packaging applications, J.

Agric. Food Chem. 66 (2018) 395–413.

[9] M. Chen, T. Runge, L. Wang, R. Li, J. Feng, X.L. Shu, Q.S. Shi, Hydrogen bonding impact on chitosan plasticization, Carbohydr. Polym. 200 (2018) 115–121.

[10] X. Ma, C. Qiao, X. Wang, J. Yao, J. Xu, Structural characterization and properties of polyols plasticized chitosan films, Int. J. Biol. Macromol. 135 (2019) 240–245.

[11] M. Matet, M.C. Heuzey, E. Pollet, A. Ajji, L. Avérous, Innovative thermoplastic chitosan obtained by thermo-mechanical mixing with polyol plasticizers, Carbohydr. Polym. 95 (2013) 241–251.

[12] A.P. Lunkov, A. V. Ilyina, V.P. Varlamov, Antioxidant, antimicrobial, and fungicidal properties of chitosan based films (Review), Appl. Biochem. Microbiol. 54 (2018) 449–458.

[13] S.A. Mir, B.N. Dar, A.A. Wani, M.A. Shah, Effect of plant extracts on the techno-functional properties of biodegradable packaging films, Trends Food Sci. Technol. 80 (2018) 141–154.

[14] W. Zhang, X. Li, W. Jiang, Development of antioxidant chitosan film with banana peels extract and its application as coating in maintaining the storage quality of apple, Int. J. Biol. Macromol. (2019), https://doi.org/10.1016/j.ijbiomac.2019.10.275.

[15] X. Zhang, J. Liu, H. Yong, Y. Qin, J. Liu, C. Jin, Development of antioxidant and antimicrobial packaging films based on chitosan and mangosteen (*Garcinia mangostana* L.) rind powder, Int. J. Biol. Macromol. 145 (2020) 1129–1139.

[16] K. Rambabu, G. Bharath, F. Banat, P.L. Show, H.H. Cocoletzi, Mango leaf extract incorporated chitosan antioxidant film for active food packaging, Int. J. Biol. Macromol. 126 (2019) 1234–1243.

[17] X. Zhang, Y. Liu, H. Yong, Y. Qin, J. Liu, J. Liu, Development of multifunctional food packaging films based on chitosan, TiO_2 nanoparticles and anthocyanin-rich black plum peel extract, Food Hydrocoll. 94 (2019) 80–92.

[18] X. Zhang, H. Lian, J. Shi, W. Meng, Y. Peng, Plant extracts such as pine nut shell, peanut shell and jujube leaf improved the antioxidant ability and gas permeability of chitosan films, Int. J. Biol. Macromol. 148 (2019) 1242–1250.

[19] Z. Li, S. Lin, S. An, L. Liu, Y. Hu, L. Wan, Preparation, characterization and anti-

aflatoxigenic activity of chitosan packaging films incorporated with turmeric essential oil, Int. J. Biol. Macromol. 131 (2019) 420–434.

[20] M. Bajić, H. Jalšovec, A. Travan, U. Novak, B. Likozar, Chitosan-based films with incorporated supercritical CO_2 hop extract: Structural, physicochemical, and antibacterial properties, Carbohydr. Polym. 219 (2019) 261–268.

[21] M. Bajić, T. Ročnik, A. Oberlintner, F. Scognamiglio, U. Novak, B. Likozar, Natural plant extracts as active components in chitosan-based films: A comparative study, Food Packag. Shelf Life. 21 (2019) 100365.

[22] K. Kõrge, M. Bajić, B. Likozar, U. Novak, Active chitosan- chestnut extract films used for packaging and storage of fresh pasta, Int. J. Food Sci. Technol. (2020), https://doi.org/10.1111/ijfs.14569.

[23] G. Biagi, I. Cipollini, B.R. Paulicks, F.X. Roth, Effect of tannins on growth performance and intestinal ecosystem in weaned piglets, Arch. Anim. Nutr. 64 (2010) 121–135.

[24] R. Amarowicz, M. Janiak, Hydrolysable tannins, in: L. Melton, F. Shahidi, P. Varelis (Eds.), Encycl. Food Chem., Academic Press, 2019: pp. 337–343.

[25] N. Echegaray, B. Gómez, F.J. Barba, D. Franco, M. Estévez, J. Carballo, K. Marszałek, J.M. Lorenzo, Chestnuts and by-products as source of natural antioxidants in meat and meat products: A review, Trends Food Sci. Technol. 82 (2018) 110–121.

[26] A. Messini, A. Buccioni, S. Minieri, F. Mannelli, L. Mugnai, C. Comparini, M. Venturi, C. Viti, A. Pezzati, S. Rapaccini, Effect of chestnut tannin extract (*Castanea sativa* Miller) on the proliferation of *Cladosporium cladosporioides* on sheep cheese rind during the ripening, Int. Dairy J. 66 (2017) 6–12.

[27] R.H. Myers, D.C. Montgomery, C.M. Anderson-Cook, Response surface methodology: Process and product optimization using designed experiments, 4th ed., John Wiley & Sons, Hoboken, 2016.

[28] G.E.P. Box, D.W. Behnken, Some new three level designs for the study of quantitative variables, Technometrics. 2 (1960) 455–475.

[29] P.C. Srinivasa, R. Ravi, R.N. Tharanathan, Effect of storage conditions on the tensile

properties of eco-friendly chitosan films by response surface methodology, J. Food Eng. 80 (2007) 184–189.

[30] T.P. Singh, M.K. Chatli, J. Sahoo, Development of chitosan based edible films: process optimization using response surface methodology, J. Food Sci. Technol. 52 (2015) 2530–2543.

[31] B. Tomadoni, A. Ponce, M. Pereda, M.R. Ansorena, Vanillin as a natural cross-linking agent in chitosan-based films: Optimizing formulation by response surface methodology, Polym. Test. 78 (2019) 105935.

[32] Y. Tao, J. Pan, S. Yan, B. Tang, L. Zhu, Tensile strength optimization and characterization of chitosan/TiO_2 hybrid film, Mater. Sci. Eng. B Solid-State Mater. Adv. Technol. 138 (2007) 84–89.

[33] R. Thakur, B. Saberi, P. Pristijono, C.E. Stathopoulos, J.B. Golding, C.J. Scarlett, M. Bowyer, Q. V. Vuong, Use of response surface methodology (RSM) to optimize pea starch-chitosan novel edible film formulation, J. Food Sci. Technol. 54 (2017) 2270–2278.

[34] P. Cazón, M. Vázquez, G. Velazquez, Composite films of regenerate cellulose with chitosan and polyvinyl alcohol: Evaluation of water adsorption, mechanical and optical properties, Int. J. Biol. Macromol. 117 (2018) 235–246.

[35] H. Liu, R. Adhikari, Q. Guo, B. Adhikari, Preparation and characterization of glycerol plasticized (high-amylose) starch-chitosan films, J. Food Eng. 116 (2013) 588–597.

[36] A. Domján, J. Bajdik, K. Pintye-Hódi, Understanding of the plasticizing effects of glycerol and PEG 400 on chitosan films using solid-state NMR spectroscopy, Macromolecules. 42 (2009) 4667–4673.

[37] G. Tondi, A. Petutschnigg, Middle infrared (ATR FT-MIR) characterization of industrial tannin extracts, Ind. Crops Prod. 65 (2015) 422–428.

[38] R.Y. Aguirre-Loredo, A.I. Rodríguez-Hernández, E. Morales-Sánchez, C.A. Gómez-Aldapa, G. Velazquez, Effect of equilibrium moisture content on barrier, mechanical and thermal properties of chitosan films, Food Chem. 196 (2016) 560–566.

[39] F. Luzi, L. Torre, J.M. Kenny, D. Puglia, Bio- and fossil-based polymeric blends and nanocomposites for packaging: Structure-property relationship, Materials. 12 (2019) 49p.

[40] B. Saberi, R. Thakur, Q. V. Vuong, S. Chockchaisawasdee, J.B. Golding, C.J. Scarlett, C.E. Stathopoulos, Optimization of physical and optical properties of biodegradable edible films based on pea starch and guar gum, Ind. Crops Prod. 86 (2016) 342–352.

Declaration of competing interests

☒ The authors declare that they have no known competing financial interests or personal relationships that could have appeared to influence the work reported in this paper.

☐The authors declare the following financial interests/personal relationships which may be considered as potential competing interests:

Highlights

- Chitosan-based film developed using chestnut extract as an active component.
- Composition of the film-forming solution linked to properties of the final film materials by RSM.
- Box–Behnken design was an effective tool in the formulation of the optimal film-forming solution.
- Level of plasticizer influenced moisture content and mechanical properties of the film material.
- Level of active component influenced the antioxidant properties of the film material.